Biomimetic Membrane System Composed of a Composite Interpenetrating Hydrogel Film and a Lipid Bilayer

*Barry Stidder, Jean-Pierre Alcaraz, Lavinia Liguori, Nawel Khalef, Aziz Bakri, Erik B. Watkins, Philippe Cinquin, and Donald K. Martin**

A simple way to form an interpenetrating hydrogel (IPH) by combining a layer-by-layer polyelectrolyte membrane with agarose is reported. The formed IPH membrane is more robust and easily manipulated compared to a polyelectrolyte membrane with the same number of layers. The IPH has good diffusion characteristics and retains the advantageous surface charge from the polyectrolyte composition that facilitates the adsorption of a stable lipid bilayer. The stable adsorption of a lipid bilayer on the IPH creates a biomimetic membrane system that is optimized for utilization in a diffusion chamber.

1. Introduction

In this work we aim to fabricate a biomimetic membrane system that includes a stable lipid bilayer and is optimized for utilization in a diffusion chamber. The novelty in this report is the adaptation of polyelectrolye multilayer films to fabricate an interpenetrating hydrogel that is permeable, of nanoscale thickness and sufficiently rigid to manipulate as a film to function as a free-standing biomimetic membrane planar support. The concept of producing semipermeable films utilizing polyelectrolytes,[1] notably with polystyrene sulfonate, was introduced in 1960 but the development of the layer-by-layer (LbL) technique of assembling polyelectrolyte films by Decher and Hong in 1991 stimulated investigation of the use of the films for many applications.[2,3] The LbL manufacturing process involves the alternate adsorption of polyelectrolytes of opposite charge onto surfaces including plastic, glass, latex, colloidal particles, bacterial or mammalian cells. Polyelectrolyte multilayer films have provided a permeable substrate to support lipid bilayers, but initially were adsorbed onto a solid supporting structure and were not free-standing.[4,5] However, the production of free-standing LbL multilayer films has definite advantages for diffusion membranes.[6] For example, a free-standing multilayer film of montmorillonite and polyelectrolyte has been formed on a cellulose acetate substrate which was then dissolved away by acetone.[7] A robust clay nanocomposite was produced by LbL assembly of PVA and montmorillonite.[8] Also, a novel approach for the fabrication of non-covalent and free-standing biopolymer assemblies has also been reported.[9] Other examples that utilize a sacrificial substrate during manufacture include the use of pH-responsive multilayer film between a substrate and the PEM, that disintegrates when the pH is adjusted to neutral[10] and the use of ion-triggered exfoliation, which breaks the electrostatic interaction between the PEM and substrate whilst keeping the integrity of the resultant films.[11]

Although black lipid bilayers have been used extensively as biomimetic membranes in physicochemical and bilayer diffusion studies since their introduction[12] in the 1960s, they have the disadvantages of relatively short lifetimes and traces of solvent residual remaining in the bilayer. The stability of a lipid bilayer can be greatly enhanced by covalently tethering the lipid molecules to a solid substrate, with the tethered layer creating a nanoscale reservoir spacer layer between the bilayer and solid substrate and removing the need for solvents during formation of the bilayer.[13] Such bilayers stabilized on solid gold surfaces are often used in electrical investigations of the bilayer properties and transport of molecules through protein channels, but the impermeabilty of the gold substrate does not make that tethered membrane system easily adaptable for diffusion chambers. The use of a polyelectrolyte film to support a lipid bilayer provides a membrane system that is permeable. Examples of previous reports of such a system include a lipid bilayer which was assembled onto polyelectrolyte-coated colloidal particles[14] or planar polyeletrolyte membranes coated onto glass.[15] Conversely, the LbL coating of liposomes provides the encapsulation of lipophilic particles inside a system named capsosomes.[16]

The simplicity and versatility of the LbL technique, especially when modified to produce hollow microcapsules,[17] allows for

Dr. B. Stidder, Dr. L. Liguori, Prof. D. K. Martin
Fondation RTRA Nanosciences
Université Joseph Fourier-Grenoble 1/ CNRS/
TIMC-IMAG UMR 5525
Grenoble, F-38041, France
E-mail: don.martin@imag.fr
J. P. Alcaraz
Université Joseph Fourier-Grenoble 1/ CNRS/ TIMC-IMAG UMR 5525
Grenoble, F-38041, France
Dr. N. Khalef, Prof. A. Bakri
Université Joseph Fourier-Grenoble 1/ CNRS/
TIMC-IMAG UMR 5525/ TheREx/ Formulation and Pharmaceutical
Formulation Engineering
Grenoble, F-38041, France
Dr. E. B. Watkins
Institut Laue-Langevin
6, rue Jules Horowitz, Grenoble, F-38042, France
Prof. P. Cinquin
Université Joseph Fourier-Grenoble 1/ CNRS/ TIMC-IMAG UMR 5525
Grenoble, F-38041, France

DOI: 10.1002/adfm.201200751

many potential biomedical applications such as micro-encapsulation, controlled drug release, biosensors as well as for tissue engineering. We have recently published a biological application with our approach utilizing the LbL technique to create a free-standing hollow microcapsule scaffold to support an ion-transporting lipid bilayer for application in an artificial cell.[18]

We present here a novel way of forming a free-standing planar polyelectrolyte multilayer film using a sacrificial substrate of low melting point agarose to produce an interpenetrating hydrogel (IPH). Our method for producing this IPH provides additional stability to the free-standing planar polyelectrolyte multilayer film by the incorporation of agarose during the fabrication of the film (**Figure 1**). The sacrificial agarose substrate is first pre-coated with a layer of poly(ethyleneimine) (PEI) which acts as a precursor to enhance the stability of the subsequent alternating polyelectrolyte multilayers.[19] Alternating layers of poly(sodium 4-styrenesulfonate) (PSS) and poly(allylamine hydrochloride) (PAH) are then deposited onto the agarose substrate using the layer-by-layer technique. Prior to the final formation of the IPH, the sacrificial substrate provides strength during manipulation and transferral of pre-formed PEM films onto a range of other substrates.

2. Results and Discussion

The robust nature of the IPH film is demonstrated in **Figure 2**, which shows a sequence of frames from a video of the removal of the bulk agarose by dissolution with hot water. For the purpose of this demonstration, the unconstrained IPH film is allowed to float in response to thermal convection currents. The remainder of the results quantify the composite nature and enhanced thickness of the IPH film compared to a classical LbL polyelectrolyte membrane. Both an elemental analysis and a thermal analysis were performed on the IPH and compared to the same mixed ratio of the pure polyelectrolytes. Tracer studies were performed to measure the diffusion coefficient of the IPH. The IPH was able to support a stable lipid bilayer, which was confirmed by impedance spectroscopy.

2.1. IPH Film Thickness Characterization

We compared the thickness of IPH films transferred onto a silicon wafer to classically prepared polyeletrolyte (PEM) films adsorbed directly onto a silicon wafer using the layer-by-layer method. Both types of films comprised 18 layers of polyelectrolytes (PEI, PSS and PAH). We utilized ellipsometry to measure the thickness of the IPH or PEM films on the silicon wafers. Both the IPH and PEM samples were dried partially at room temperature following an identical protocol before the ellipsometry measurements. The thickness of the PEM film adsorbed directly on silicon was 32 ± 1 nm (n = 8). Neutron reflectivity measurements were performed on fully hydrated PEM films and indicated that the thickness of the PEM films was 33 ± 1 nm (**Figure 3**), with the error on the thickness based on the amount of change in the chi-square by 1 in the modelling. The neutron reflectivity measurement of thickness confirmed that the procedure for the ellipsometry

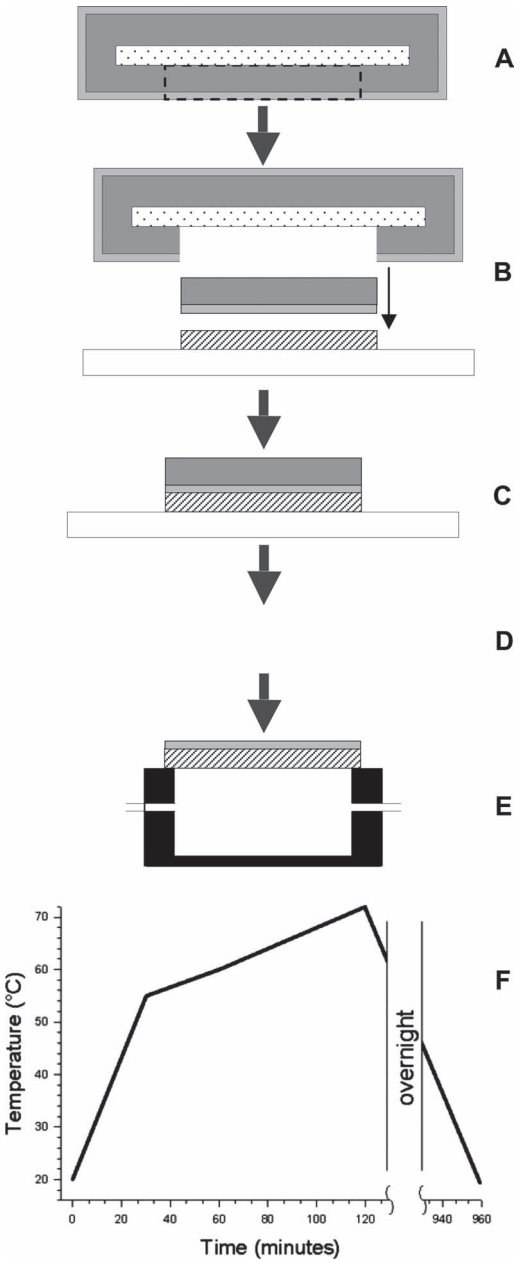

Figure 1. Schematic of the fabrication method for the free-standing polyelectrolyte film using the sacrificial agarose support. The various materials are identified by the different shadings, as polystyrene microscope slide (stippled), agarose (dark gray), polyelectrolyte film (light gray), and track-etched polycarbonate (diagonal lines). The larger unfilled rectangle in B, C, and D represents the glass microscope slide used as a base during the fabrication procedures. A) The polyelectrolyte film is adsorbed using the LbL method onto agarose, which has been coated onto a polystyrene microscope slide. The LbL adsorption process is assisted by a robot to control the reproducibility of formation of the polyelectrolyte film between batches. B) A section of agarose+polyelectrolyte is cut from the coated microscope slide. C) The section of agarose+polyelectrolyte is placed onto a piece of track-etched polycarbonate. D) The bulk agarose is removed from the polyelectrolyte film by a slow heating protocol in a water bath. E) The polyelectrolye+polycarbonate is placed into the diffusion chamber (black). F) The slow heating protocol to remove the bulk agarose. The heat was turned on at 0 min and turned off at 120 min, to allow cooling of the water bath overnight.

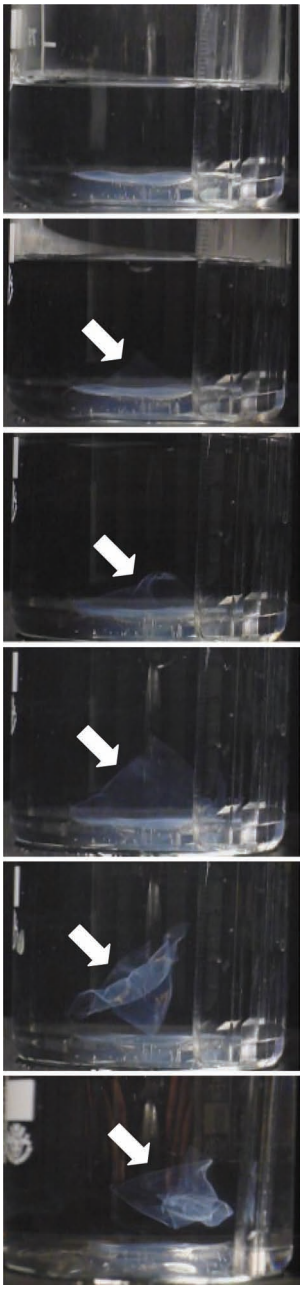

Figure 2. Demonstration of the robust nature of the composite agarose/polyelectrolyte membrane. The following sequence of frames from a video demonstrates that the unconstrained membrane floats from the bulk agarose in response to sequential aliquots of hot (90 °C) Milli-Q water. This was achieved by placing a portion of the polyelectrolyte-coated agarose PEM film side up in a glass beaker containing 60 °C Milli-Q water. In this demonstration no polyvinylchloride mask was used to restrain the PEM film. The PEM film is indicated by the white arrows and it keeps its integrity, but is prone to folding in response to the thermal convection currents from the addition of the hot aliquots of Milli-Q water.

measurements produced an accurate measurement of the film thickness. The thickness of the IPH film, using ellipsometry, was found to be much thicker having an average value of 278 ± 2 nm (n = 8).

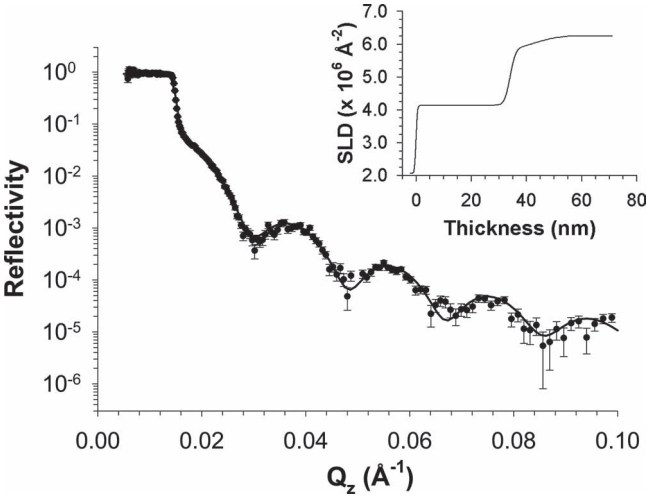

Figure 3. Neutron reflectivity data and corresponding model fit for 18 layers of PSS/PAH polyelectrolyte at the silicon/D_2O interface. Data was modeled using a single, homgoneous layer to describe the polyectrolyte film and an additional diffuse layer representing the outermost solvated polyectrolyte layer. The inset displays the scattering length density profile corresponding to the model. The thickness of the homogenous region of the film was 34.5 nm.

2.2. Elemental Analysis

Elemental analysis confirmed the presence of agarose in the IPH film. The agarose enters the IPH film either during the heating process to remove the bulk sacrificial agarose layer or during the layer-by-layer dipping process and interpenetrates the polyelectrolytes to produce the IPH film. The elemental monomeric composition of the polyelectrolytes are $C_8H_7O_3SNa$ for PSS, C_3H_8NCl for PAH, $C_{24}H_{59}N_{11}$ for PEI and $C_{12}H_{18}O_9$ for agarose. The elemental analysis of a control mixture of PSS, PAH and PEI (ratio 9:8:1), low melting point agarose and of the IPH film formed from 18 LbL PEM are shown in **Table 1**. The carbon and oxygen content of the IPH film is considerably higher than that of the control mixture of polyelectrolytes. It is likely that the increased carbon content is due to the residual agarose that is incorporated with the PEM to form the IPH film after the water bath treatment. This aspect of the elemental

Table 1. Elemental analysis of the IPH film, agarose, and of control mixtures of polyelectrolytes. The values are presented as weight-percentage composition of the material. The column "other" represents the combined weight-percentage of Na and Cl present in the samples. There is a greater amount of Na and Cl present in the Control PE Mix because this is the solution that results from combining PAH, PSS, and PEI. In that case each PAH molecule brings one Cl and each molecule of PSS brings one Na. Conversely, the NaCl is leached from the IPH film during the process of manufacture and the low level of Na and Cl in the agarose is insignificant compared to the C and O.

	Carbon	Oxygen	Nitrogen	Sulphur	Hydrogen	Other
IPH film	48.8	24.3	5.2	8.3	6.6	6.8
Control PE mix	37.8	19.8	6.9	7.7	6.2	21.6
Agarose	44.2	48.0	<0.1	<0.1	6.0	1.6

analysis suggests strongly that the increased thickness of the IPH film is due to the incorporation of agarose.

The higher content of oxygen in the IPH film could be due to the presence of bound water in the gel.[20] This is consistent with the elemental analysis showing that the measured oxygen content of the control mixture of polyelectrolytes (PSS, PAH, and PEI) was higher than the predicted oxygen content based on the chemical formulae. Although the control mixture of polyelectrolytes was dried for 3 days at 45 °C it is likely that water molecules remain bound to the polyelectrolytes.[20] The thermal analysis also confirmed the presence of water in the samples (see Section 2.3).

Nitrogen is exclusively present in PEI and PAH, and sulfur in PSS. Thus, as has been previously considered,[21] the ratio of nitrogen to sulfur provides an estimation of the ratio between of the monomeric units of cationic polyelectrolytes (PEI and PAH) to the anionic polyelectrolyte (PSS). Taking into account that the IPH film comprises 9 layers of PSS, 8 layers of PAH and 1 layer of PEI, and assuming that each dip into each polyelectrolyte adsorbs the same amount of N and S atoms, then we calculate the N:S ratio to be 0.90. The measured N:S ratio is 0.9 for the control mixture of polyelectrolytes and thus agrees with the calculated value. However, the measured N:S ratio is 0.62 for the IPH film which provides further evidence that the IPH film contains agarose, and that the IPH comprises approximately 30% agarose.

2.3. Thermal Analysis

We confirmed the formation of an interpenetrating hydrogel with the technique of DSC and showed the IPH had a transition temperature different to either agarose or the polyelectrolytes alone. Three thermal events were observed for the measured samples, which occurred between 70 °C and 105 °C, between 130 °C and 190 °C and between 245 °C and 290 °C (**Figure 4**A). The expected endothermic gel-sol transition is observed for the agarose sample at 87 °C. The IPH is the only other sample that shows a similar endotherm at 82 °C (Figure 4B). An endotherm around 130 °C to 190 °C was observed for all the measured samples. The pure compounds PSS, PAH and the agarose free physical mixture of PSS-PAH showed small and broad endotherms while agarose and the IPH

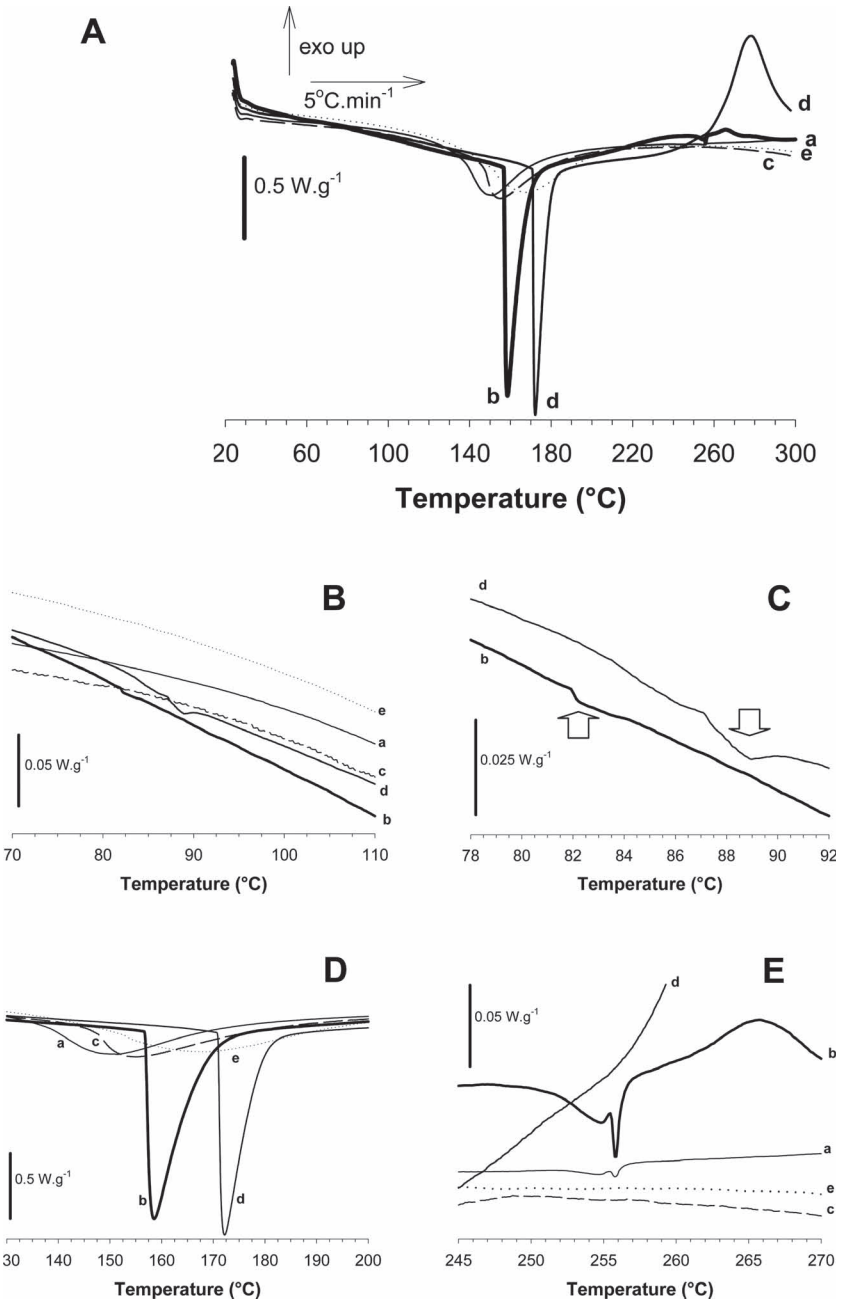

Figure 4. Thermal analysis of the IPH and related compounds. For all themograms exothermic heat flux is in the upward direction and the scan rate was 5 °C min^{-1}. A) DSC thermograms of a) mixture PAH + PSS, b) IPH, c) PSS, d) agarose, and e) PAH, which show three main thermal events that occur between 70 °C and 110 °C, 130 °C and 200 °C and between 245 °C and 290 °C. B) Zoom on the thermograms between 70 °C and 110 °C, which indicates an endotherm due to agarose melting on the thermograms for the pure agarose and the IPH. C) Zoomed view of the thermograms between 78 °C and 92 °C to show more clearly the endotherm due to agarose melting for the pure agarose and the IPH. D) Zoomed view of the thermograms between 130 °C and 220 °C showing an endotherm due to the evaporation of the water in the samples. E) Zoomed view of the thermograms between 245 °C and 270 °C, which indicates a similar thermal behavior for the IPH and the mixture of PAH and PSS. Only the IPH and the mixture of PSS and PAH show a similar endotherm attributed to the interaction between PSS and PAH. At 256 °C only IPH and pure agarose show a similar exotherm due to the agarose decomposition.

showed similar bigger and sharper endotherms (Figures 4A,C). Those endotherms are attributed to evaporation of sorbed water from the samples, as samples were voluntarily not dried prior analysis. At 248 °C both IPH and the physical mixture of PSS-PAH undergo similar endotherms not observed in the pure compounds (Figure 4D). Commenting on this phenomenon is beyond the scope of this paper, however we attribute this to the interaction between solid PSS and PAH known to occur in the presence of bulk water. Further investigations will be carried out to clarify this hypothesis.

Between 256 °C and 290 °C, the pure agarose shows a large exotherm (Figure 4A) due to its decomposition (visual observation after the scanning showed that the sample was burned). A similar decomposition was also reported for Agar samples.[22] The IPH was the only sample that showed a similar exotherm at the same onset temperature (Figure 4A,D).

The IPH prepared on the agarose substrate is the only analyzed sample that shows similar thermal behavior to the pure agarose sample. The observations of the thermal behavior to support that conclusion are a) at 81 °C, which is 5 °C below the pure agarose gel-sol transition, but such a shift to a lower value has been reported earlier for agarose-poly(acrylamide) based interpenetrating hydrogels,[23] b) around 150 °C IPH showed a large and sharp endotherm which were similar to the agarose sample and attributed to the water content evaporation while PSS, PAH and the agarose free physical mixture of PSS-PAH showed much smaller and broader endotherms, and c) at 256 °C IPH showed a similar decomposition exotherm[22] as the pure agarose sample while the other samples did not show such exotherm.

The thermal events indicate that agarose is present in the IPH. The similar onset decomposition temperature of pure agarose and IPH suggests that some remaining free agarose is present in the IPH. However, the shift in the gel-sol temperature suggests that polyelectrolyte polymers form an interpenetrating hydrogel with agarose, which is an interpretation supported by the work of Fernández et al.[23]

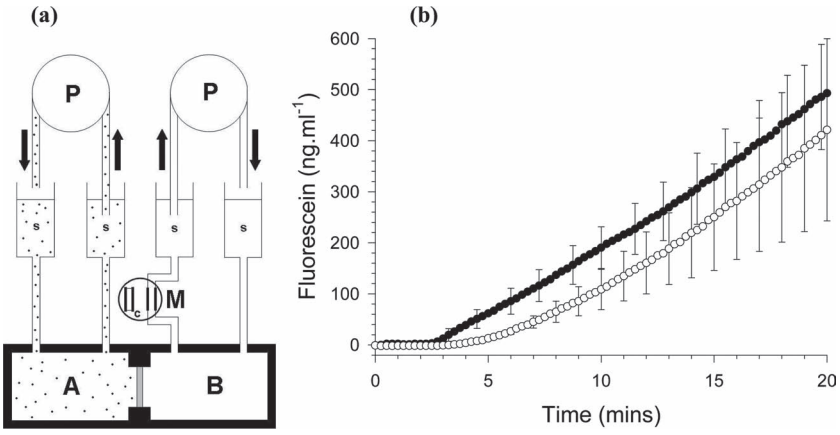

Figure 5. a) Method of conducting the diffusion experiment. Note that the lipid bilayer is not covering the IPH film for this diffusion experiment. The membrane is sandwiched between the two half-chambers of the diffusion apparatus (A and B). The same peristaltic pump (P) closed the system to provide a gravity-driven flow-rate of 800 µL.min^{-1} simultaneously through both the chambers A and B from a bank of syringes (s). The solid arrows indicate the direction of flow of the test solutions in the diffusion apparatus. The tracer for the diffusion is fluorescein. The assay for the diffusion is the measurement of fluorescence in the solution from chamber B that flowed through a borosilicate glass microcapillary tube inserted in the tubing of the pump system. To control for signal variations on-the-fly the fluorescence of a blank solution (c) in a closed borosilicate glass capillary was measured simultaneously with the the solution flowing in chamber B. For that measurement the microcapillary tubes are fixed onto the stage of a fluorescence microscope, as illustrated in the diagram by the thicker lines inside the circle labelled M. The fluorescence of the solutions flowing through both glass microcapillary tubes are recorded continuously by a computer-controlled camera attached to the fluorescence microscope. At the start of each experiment the same buffer solution is pumped through both chambers A and B. The diffusion experiment is performed by first loading a high concentration (1 mg mL^{-1}) of fluorescein in the buffer solution of the pumping system for chamber A, which approximates an infinitely high supply concentration for the diffusion process. The permeability of the supported polyelectrolyte is calculated from the increase in fluorescence of the solution pumped through chamber B. b) Increase in fluorescein concentration in chamber B of the diffusion apparatus. The open symbols represent diffusion measurements with the combined IPH film and polycarbonate supporting membrane. The closed symbols represent diffusion measurements with the polycarbonate supporting membrane alone.

2.4. Diffusion Through the IPH Film

The IPH film was supported by a porous polycarbonate membrane (track-etched 100 nm pores) for further utilization in diffusion chambers. In separate experiments we measured the flux of fluorescein through the polycarbonate supporting membrane and then the diffusion through the combined IPH film and the polycarbonate supporting membrane (**Figure 5**). For both samples the dead-volume in the tubing results in a dead-time from the introduction of fluorescein into chamber A and the appearance of fluorescein under the microscope in chamber B. The dead-time is approximately 3 min (191 s) when measured with the polycarbonate membrane and 5 min (321 s) for the combined IPH film and polycarbonate membrane. The 2 min difference between the two samples is explained by the IPH film functioning as a delay compartment. After the IPH film is saturated with the fluorescein tracer then the diffusion continues through the combined membrane system. That type of response is unable to be observed in diffusion measurements using Na^+ as the tracer since that ion is already present in the polyelectrolytes during the fabrication process.

The permeability coefficient (P) of the IPH film was calculated from the measurements of the flux of fluorescein according to the expression of Fick's law on passive diffusion

$$P = \frac{V}{AC_a}\left(\frac{dC_b}{dt}\right) \quad (1)$$

where V is the volume of the receiving chamber B (0.15 mL), A is the surface area of the IPH film for diffusion in the chambers (0.385 cm^2), C_a is the concentration of fluorescein in the

donor chamber A (1000 ng mL^{-1}), and dC_b/dt is the slope of the linear portion of Figure 5.

The diffusion coefficient (D) for the IPH film was calculated from

$$D = Pl \quad (2)$$

where l is the thickness of the IPH film (278 nm).

The permeability coefficient for the IPH film is $P = 2.70 \times 10^{-4}$ cm s^{-1}. The diffusion coefficient for the IPH film is $D = 7.51 \times 10^{-9}$ cm^2 s^{-1}.

2.5. Formation of Lipid Bilayer on IPH

After the IPH on track-etched membrane had been sealed into the diffusion cell an additional layer of PSS was absorbed onto the IPH to ensure the outer layer, for contact with the lipid bilayer, was negatively charged. The lipid bilayer was formed on the IPH by the addition of liposomes of DOPC:DOPE:DMPA:cholesterol in the molar ratio of 40:20:20:20. That ratio provides a model for the lipid and sterol types present in a typical plasma membrane. The formation of the lipid bilayer was followed by impedance spectroscopy via platinum electrodes in the upper and lower chambers of the diffusion cell.

Figure 6 shows that the lipid bilayer formed from the addition of the liposomes increased the impedance of the biomimetic membrane system and that it was predominately resistive in nature at frequencies less than 1 Hz. At 1 Hz the impedance of the IPH and the polycarbonate support is 1.41×10^5 Ω, which interestingly is in the same order of magnitude

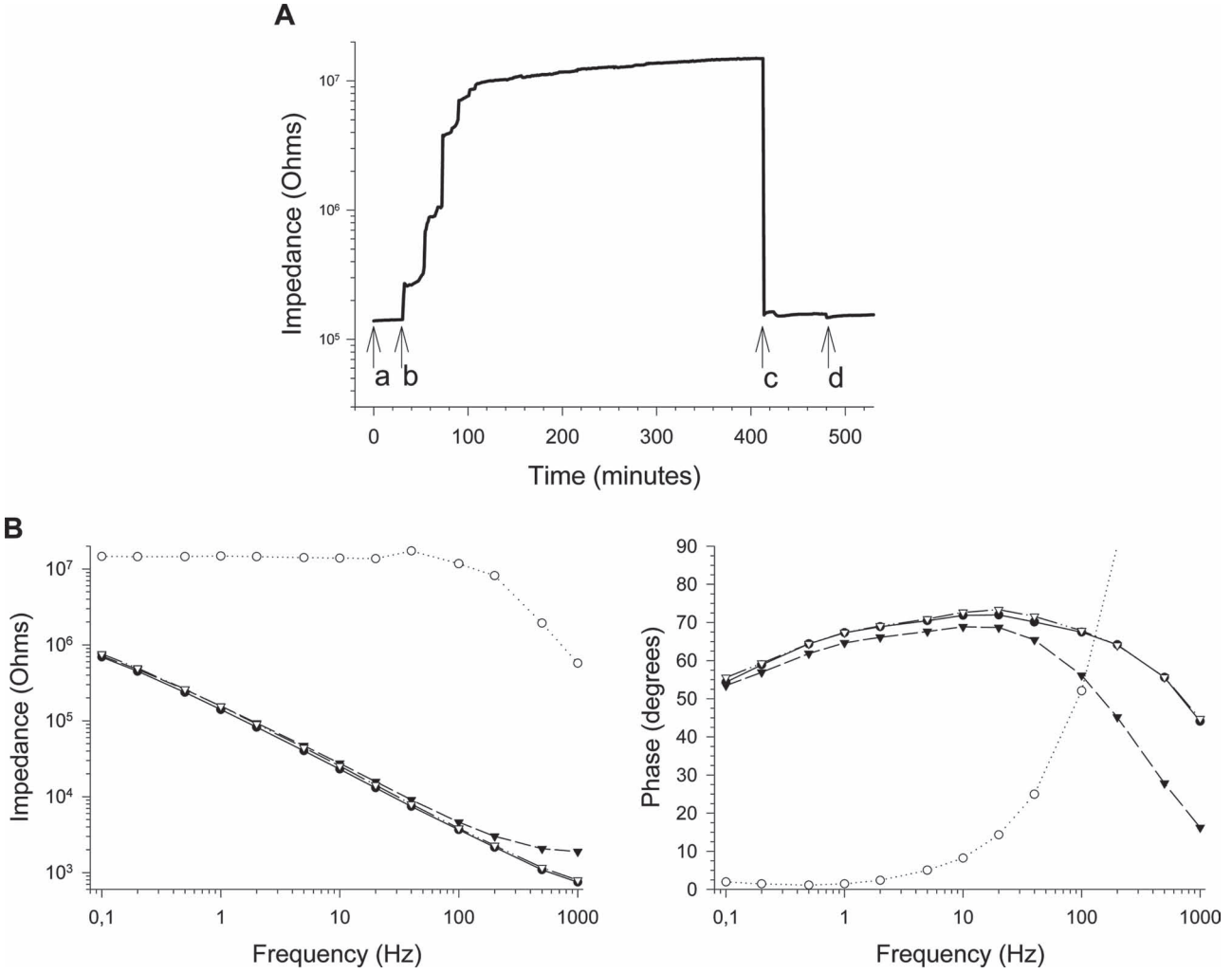

Figure 6. A) Electrical impedance of the composite biomimetic membrane system coated with a lipid bilayer measured at 1 Hz. a) Impedance of the composite biomimetic membrane superfused by NaCl buffer solution. b) Addition of liposomes to form a lipid bilayer. c) Addition of pure ethanol to remove the lipid bilayer from the composite biomimetic membrane system. d) Replacement of superfusing solution with original NaCl buffer solution (washout). B) Bode plots of the impedance and phase of the biomimetic membrane system, recorded when the impedance and phase had reached steady-state. In both plots the symbols represent the conditions of: ● impedance of the composite biomimetic membrane superfused by NaCl buffer solution, ○ addition of liposomes to form a lipid bilayer, ▼ addition of pure ethanol to remove the lipid bilayer from the composite biomimetic membrane system, and ▽ impedance of the composite biomimetic membrane superfused by NaCl buffer colution (washout).

as the impedance reported (8×10^5 Ω) for a hydrogel film of 5 μm in thickness.[24] At 1 Hz, the impedance of the combined biomimetic system of the lipid, IPH and polycarbonate is 1.47×10^7 Ω. The IPH support provides a system for a stable lipid bilayer to be used in a diffusion chamber. For example, the impedance recordings indicate the lipid bilayer was stable when we deliberately stopped the experiment after 5 h by removing the lipid bilayer using ethanol (Figure 6).

3. Conclusions

We report the production of an IPH membrane by combining polyelectrolyte films produced using the Layer-by-Layer technique with a sacrificial agarose substrate. The IPH membrane is sufficiently robust to be manually transferred to one side of a supporting porous scaffold membrane, such as a track-etched polycarbonate membrane, to enable construction of a biomimetic membrane system that includes a supported lipid bilayer for practical use in a diffusion chamber. By comparison, for the purpose of creating an equivalent continuous supporting polyelectrolyte membrane, the formation of layer-by-layer polyelectrolyte films directly on one side of track-etched polycarbonate membranes is not possible due to the high prevalence of nanopores that penetrate the polycarbonate membranes. In such a case the polyelectrolyte will coat the top and bottom surfaces and also the inside of the nanopores but not form a continuous membrane to span the pores. However, that type of utilization of polyelectrolytes can have an advantage for the alternative specific purpose of utilizing the pores of the track-etched membrane as a template for producing nanotubes of polyelectrolyte.[25]

We chose agarose as the sacrificial substrate due to its simplicity of removal with no requirement for additional chemical solvents. Chemical solvents have been reported for other types of sacrificial substrates, including, for example, free-standing multilayer films of montmorillonite and polyelectrolyte that have been formed on a cellulose acetate substrate which was then dissolved away by acetone.[26] Other examples are the use of pH-responsive multilayer film between a substrate and the polyelectrolyte membrane, that disintegrates when the pH is adjusted to neutral[27] and the use of ion-triggered exfoliation, which breaks the electrostatic interaction between the polyelectrolyte membrane and the substrate whilst maintaining the integrity of the resultant films.[28]

Using the agarose-sacrificial method we fabricated an IPH that comprised 18 single polyelectrolyte layers. The increased thickness due to the incorporation of the agarose in the IPH provides an advantageous production method compared to increasing the number of layers in the more classical layer-by-layer production technique. For example, to create a 280 nm thick film of pure polyelectrolyte would take hundreds of dips in oppositely charged solutions. The use of a sacrificial agarose substrate also overcomes the problems that would occur when trying to manoeuvre this type of membrane into a diffusion cell, especially for the requirement to keep it flat.

In our studies of the diffusive properties of IPH on a porous track-etched polycarbonate support fluorescein was used as a tracer to investigate the diffusion in the combined membrane system. For example, the kinetics of the charged fluorescein diffusing through the system provided information about the extent to which the IPH provided a passive delay in the diffusion in the combined system. Our use of a sacrificial IPH membrane laid onto the porous track-etched polyelectrolyte scaffold allowed our diffusion experiments to directly compare the control sample of track-etched polycarbonate membrane (100 nm porosity) with a track-etched polycarbonate membrane with an IPH film on top of it. This differs from other diffusion studies of polyelectrolyte membranes in that the IPH is only on one side, the polyelectrolyte has not penetrated the nanopores of the supporting track-etched porous membrane, and the IPH is not attached to the membrane such as in the studies reported by Dirieh Egueh et al., who dipped both sides of a polyethersulfone anisotropic membrane.[29] We chose fluorescein as the tracer molecule because it allows quantitative optical measurements of diffusion and is not present inside the IPH before the measurement. This provides a more direct observation that the IPH functions as a compartment in the diffusion pathway, unlike the electrical measurement of streaming potential used in a previous study,[30] and that once saturated with the diffusing species the IPH membrane does not retard the diffusion of the species.

There is no disadvantage on restricting diffusion through the biomimetic membrane system we report due to the incorporation of the agarose in the IPH. The diffusion coefficient of $D = 7.51 \times 10^{-9}$ cm^2 s^{-1} measured on the IPH compares favorably with previous reports of the diffusion properties of polyelectrolyte membranes and of agarose membranes. Indeed, although there is a low diffusion coefficient on the order of 10^{-15} cm^2 s^{-1} for the transport of fluorescent molecules that are bound electrostatically to polyelectrolyte membranes,[31] the diffusion coefficient of the redox molecule ferricyanide through a 10 bilayer PDADMA/PSS polyelectrolyte membrane at room temperature is around 2×10^{-9} cm^2 s^{-1}.[32] The diffusion coefficient for KCl through a 6 bilayer PAH/PSS film adsorbed onto a polyethersulfone anisotropic membrane is 10.62×10^{-9} cm^2 s^{-1}.[29] The diffusion coefficient of 4×10^{-7} cm^2 s^{-1} for BSA protein through a 5% w/w agarose gel[33] is larger than for the polyelectrolyte membrane, and is probably due to the uncharged nature of the agarose gel.

The IPH has the advantage of being more robust and easily manipulated compared to a polyelectrolyte membrane of the same number of layers, but the IPH retains the advantage of a surface charge from the polyectrolyte composition in order to facilitate the adsorption of a lipid bilayer. The combination of the IPH and a supported lipid bilayer provides an impedance of a similar order to a tethered lipid bilayer of a similar area on a solid support[34] or black lipid membranes suspended over micrometer-sized apertures in filter membranes.[35] The distinct advantage of the IPH biomimetic membrane system we describe is the easy construction of a permeable biomimetic membrane system for use in diffusion chambers. For example, this biomimetic membrane system provides an alternative to a black-lipid-membrane system since the formation of the supported lipid membrane does not require specific solvents.

4. Experimental Section

Materials: Poly(ethyleneimine) (Sigma-Aldrich, P3143), poly(sodium 4-styrenesulfonate) (Sigma-Aldrich, 243051), poly(allylamine

hydrochloride) (Sigma-Aldrich, 283223), sodium chloride (Sigma-Aldrich, 10094482), Fluorescein sodium salt and cholesterol (Avanti Polar Lipids, 700000P) were purchased from Sigma-Aldrich, France and used as received. Low melting temperature agarose (Type LM-3, ref. 1670, lot H111221) was purchased from Euromedex, France and had a manufacturer's stated gelling temperature (1.5%) of 24.5 °C, a stated melting temperature (1.5%) of 65.3 °C and a stated gel strength (1.5%) of >400 g cm^{-2}. Ultrapure water was of Milli-Q grade. Polycarbonate track-etched membranes of 100 nm pore size (Whatman, 7060-2501) were purchased from Whatman International Ltd. 1,2-dioleoyl-sn-glycero-3-phosphocholine (Avanti Polar Lipids, 850375), 1,2-dioleoyl-sn-glycero-3-phosphoethanolamine (Avanti Polar Lipids, 850725) and 1,2-dimyristoyl-sn-glycero-3-phosphate (sodium salt) (Avanti Polar Lipids, 830845) were purchased from Avanti Polar Lipids, USA and used as received.

Layer-by-Layer Fabrication of Polyelectrolyte Film on Agarose-Coated Substrates: The novel polyelectrolyte fabrication process is illustrated in Figure 1. The low melting temperature agarose was dissolved in Milli-Q water to a concentration of 5%. Polystyrene microscope slides were coated thoroughly on all sides with the agarose to a thickness of 1.5 mm. It is necessary to coat both sides of the slide to stop the agarose detaching from the slide. Polyelectrolyte solutions of PSS and PAH (1 mg mL^{-1}) were made with a NaCl salt solution (0.5 M) and PEI (1 mg mL^{-1}) with ultrapure water. The agarose-coated slides were then dipped for 20 minutes in the PEI solution, followed by rinsing in ultrapure water. To ensure reproducibility an Epson Accusembler robot was customized and programmed to perform the layer-by-layer procedures to adsorb 17 alternate single layers of PSS and PAH, with rinsing steps in between. The agarose-coated microscope slides were loaded into a custom-built slide holder for the Epson Accusembler robot, that contained 6 slides. The robot dipped the slide-holder alternatively in solutions of PSS and PAH for 5 minutes to form the required number of adsorbed layers. Between each dip the slides were rinsed for 5 min each and sequentially in two different containers of ultrapure water to remove excess polyelectrolyte and prevent contamination of the polyelectrolyte solutions. The finished samples were then stored in Milli-Q water until use. The time for storage before use was kept to a minimum, with the agarose typically removed within 4 days.

Removal of Agarose and Transferral of Polyelectrolyte Film onto Track-Etched Membranes: Track-etched membranes with a pore size of 100 nm were used as a passive support for the polyelectrolyte films. As illustrated in Figure 1, a section of the agarose coated with the polyeletrolyte film was placed on the track-etched membrane with the orientation PEM-film down. The section was cut so as to be larger than than the surface area of the area for permeation in the diffusion apparatus. A polycarbonate mask fabricated from a 1 mm thick sheet of polyvinylchloride was used to constrain the edges of the PEM-film to avoid the film floating off the track-etched membrane during the following heating protocol. Note that the central area of the PEM-film, the target area for adsorption of the lipid bilayer in the diffusion apparatus, was not constrained. The agarose was removed from the PEM film by heating in a water bath filled with Milli-Q water according to the protocol shown in Figure 1. It is important that the water bath is heated slowly to minimize thermal convection currents that could disrupt the PEM film. The volume of the water-bath was infinitely greater than the volume of the bulk agarose attached to the PEM film, and the bulk of the agarose disperses in the water to leave an intact polyelectrolyte film on the membrane with the outer layer being the positively charged PEI. The composite nature of the remaining agarose/polyelectrolyte in the membrane provided it sufficient strength so that is did not tear (see also illustration of the membrane integrity in Figure 1). The agarose/polyelectrolyte membrane was kept immersed in Milli-Q water until being placed in the diffusion apparatus. This method can also be used to transfer the agarose/polyelectrolyte films to a range of substrates.

Formation of Lipid Bilayer on PEM: The PEM on track-etched membranes were transferred into the diffusion cell and an additional layer of PSS was adsorbed on top of the PEM to ensure a negative outer surface for lipid bilayer adsorption. The lipid bilayer was formed on one side of the PEM via vesicle fusion. Vesicles of DOPC:DOPE:DMPA:cholesterol (molar ratio of 40:20:20:20) were made by first mixing the lipids in chloroform followed by evaporation. The lipids were then suspended in TRIS buffer (50 mM pH 7.5) and extruded through 100 nm diameter pores to form single unilamellar vesicles (SUV), which were added to the solution that superfused the PEM in the diffusion chamber.

Elemental Analysis of PEM Composite Film: 10 mg of PEM film was prepared by transferring PEM onto glass microscope slides from agarose sacrificial substrates, which were then dried at 45 °C for 3 days. The PEM was removed from the slides using a spatula. A control sample of pure PEI/PSS/PAH was made by mixing a ratio representative of the number of layers deposited in ultra pure water (9:8:1 of PSS/PAH/PEI). The sample was then treated in the same way as the PEM film. A pure sample of low melting agarose was also prepared. The samples were measured by the Service Central d'Analyse CNRS, Solaize, France using CNRS-built microanalysers according to the CNRS protocol RC-E2-01. The measurements were of the% composition by mass of the elements in the samples, to a precision of ±0.3%.

Thermal Analysis of PEM Composite Film: Thermal analysis was performed with differential scanning calorimetry (DSC, TA instrument 2920, France). The instrument was calibrated using pure indium. Separate thermal analysis was performed on samples of the PEM composite membrane, the original pure compound PSS, the original pure compound PAH, the original pure compound agarose, and a 50/50% (w/w) physical mixture of PSS and PAH prepared in the absence of agarose (*Mix PAH-PSS*). For each analysis a small amount of the the typical 1 to 3 mg of sample (typically in the range 1 mg to 3 mg) was precisely weighed and scanned from 25 °C to 300 °C at 5 °C min^{-1}. Samples were stored under normal atmospheric RH conditions in order to detect any gel-sol transition for those samples containing agarose.[23]

Diffusion Measurements Procedure: The diffusion apparatus is illustrated in Figure 5. The measurements were performed in a custom-built diffusion cell consisting of two half chambers, each of 150 µL volume. The sample (either track-etched membrane alone or with PEM film on top of it) was placed between the chambers under water to avoid disruption of the PEM film and formation of air bubbles. The sample was clamped with o-rings to seal the apparatus. Measurements were performed in two chambers concurrently as shown in Figure 5. The syringes were filled with water for chamber B and fluorescein (1 mg mL^{-1}) for chamber A. Gravity flow at a rate of 800 µL min^{-1} was used to circulate and stir the 2 solutions in the same manner. Each half-chamber and tubing contained a total volume of 1800 µL ("dead-volume"). A peristaltic pump was connected to the syringes to close the circulation system. Fluorescence was read under an Axiovert 135 fluorescence microscope (Carl Zeiss, Jena, Germany) through a glass capillary connected to the chamber B. Data collection was performed with the MetaVue Imaging System which was programmed to collect an image of the sample capillary and reference capillary every 15 s. Analysis of the images was performed with ImageJ software. The output of the fluorescence camera (A.U. = absorption units) was calibrated using a 2-point calibration procedure by measuring the fluorescence of a blank solution (200 A.U.) and a solution containing fluorescein (10 µg mL^{-1}) to achieve the maximum fluorescence recordable (1500 A.U.).

Impedance Spectroscopy: The technique of electrical impedance spectroscopy was used to measure the conductance properties of the biomimetic membrane system placed in a diffusion apparatus. The impedance spectrum was obtained by applying to the tethered lipid bilayer membrane an AC excitation signal of 30 mV p-p amplitude in a frequency sweep from 0.1 Hz to 1 kHz over a period of 60 s (SDXTetheredMembranes Pty Ltd, Australia). The AC excitation signal was applied across platinum working and counter electrodes inserted in the two chambers of the diffusion apparatus, with no applied DC offset to the biomimetic membrane system.

Adsorption of Polyelectrolyte Layers Directly onto Silicon Wafers: The silicon wafers were cleaned by treatment with hot piranha solution (35 wt% H_2O_2/85 vol% H_2SO_4 (1:1) v/v, 80 °C) for 20 min. That cleaning procedure was performed with extreme caution under a

flow-hood. After removal from the piranha solution the silicon wafers were immediately rinsed extensively in ultrapure water. A precursor of PEI followed by the required number of PSS and PAH layers were adsorbed in using the method detailed above for the agarose slides. The samples were then stored under water until use, with the storage time typically of 4 days.

Ellipsometry: Two types of samples were measured. PEM deposited onto silicon directly using the layer-by-layer technique and PEM free floating film transferred by the sacrificial agarose method described in this article. Excess surface water was blotted from the films using lint-free tissue paper. Measurements of PEM thickness were performed in-air using a rotating quarter wave plate ellipsometer, operating at 660 nm and an angle of 75° (custom-built at ILL, software by Ellipso Technology). A refractive index of 1.47 was used for the PEM to calculate the thickness.[36] For each sample studied, multiple measurements were taken randomly at different locations across the film.

Neutron Reflectivity: The thickness of 18 layers of PSS/PAH polyelectrolyte adsorbed directly on silicon's native oxide was measured at the solid/liquid interface in deuterated water using specular neutron reflectivity (SNR).[37,38,39] For SNR, incident neutrons are elastically and specularly scattered from a planar sample at small glancing angles. Reflectivity is defined as the ratio of incident to reflected neutrons and is measured as a function of the momentum transfer vector (Q_z), with $Q_z = 4\pi\sin(\theta)\,\lambda^{-1}$. SNR is sensitive to the nuclear scattering length density of the sample and probes the in-plane averaged structure perpendicular to the surface. SNR is particularly sensitive to the thickness and composition of the layered structure, and the roughness of the interfaces. Measurements were performed on FIGARO, the time-of-flight horizontal reflectometer at the high flux reactor of the Institut Laue-Langevin (ILL, Grenoble, France). Using 2 Å to 20 Å wavelength range and two incident angles of 0.624° and 3.78°, data were collected up to 0.10 $Å^{-1}$ with a resolution of ≈6.5% dQ_z/Q_z. Data analysis was performed using the standard layered box-model,[29] where the simulated reflectivity was fitted to the measured reflectivity using chi-square minimization in motofit software (WaveMetrics, Oregon, USA).

Acknowledgements

B.S. and J.P.A. contributed equally to this work. The authors thank the Institut Laue Langevin (ILL) for provision of beam-time and Dr. Giovanna Fragneto from the Partnership for Soft Condensed Matter (PSCM) for valuable discussions concerning the planning of the experiments. They also thank Ida Berts from the Partnership for Soft Condensed Matter (PSCM) for instruction on the use of the PSCM ellipsometer, and Dr. Cyrille Rochas from Centre de Recherches sur les Macromolecules (CERMAV, CNRS UPR 5301) who provided helpful discussions on agarose. The authors thank the Réseau Thématique Recherche Avancé (Fondation Nanosciences) and the Pôle CSVSB (Université Joseph Fourier) for financial support of this research. D.K.M. was supported by a Chaire d'Excellence from the Fondation Nanosciences, B.S. was supported by a Postdoctoral Fellowship from the Pôle CSVSB, and L.L. was supported by a Postdoctoral Fellowship from the Fondation Nanosciences.

Received: March 17, 2012
Published online: June 14, 2012

[1] M. Mindick, H. I. Patwelt, *US Patent 2957206* **1960**.
[2] G. Decher, J. D. Hong, *Makromol. Chemie–Macromol Symp.* **1991**, *46*, 321.
[3] G. Decher, J. D. Hong, J. Schmitt, *Thin Solid Films* **1992**, *210/211*, 831.
[4] R. Kügler, W. Knoll, *Bioelectrochemistry* **2002**, *56*, 175.
[5] J. Chen, R. Köhler, T. Gutberlet, H. Möhwald, R. Krastev, *Soft Matter* **2009**, *5*, 228.
[6] M. Nolte, A. Fery, *IEE Proc. Nanobiotechnol.* **2006**, *153*, 112.
[7] A. A. Mamedov, N.A Kotov, *Langmuir* **2000**, *16*, 5530.
[8] P. Podsiadlo, A. K. Kaushik, E. M. Arruda, A. M. Waas, B. S. Shim, J. Xu, H. Nandivada, B. G. Pumplin, J. Lahann, A. Ramamoorthy, N. A. Kotov, *Science* **2007**, *318*, 80.
[9] D. Mertz, P. Tan, Y. Wang, T. K. Goh, A. Blencowe, F. Caruso, *Adv. Mater.* **2011**, *23*, 5668.
[10] S. S. Ono, G. Decher, *Nano Lett.* **2006**, *6*, 592.
[11] Y. Ma, J. Sun, J. Shen, *Chem Mater.* **2007**, *19*, 5058.
[12] P. Mueller, D. O. Rudin, H. T. Tien, W. C. Wescott, *Nature* **1962**, *194*, 979.
[13] B. A. Cornell, V. L. B. Braach-Maksvytis, L. G. King, P. D. J. Osman, B. Raguse, L. Wieczorek, R. J. Pace, *Nature* **1997**, *387*, 580.
[14] S. Moya, W. Richter, S. Leporatti, H. Bäumler, E. Donath, *Biomacromolecules* **2003**, *4*, 808.
[15] G. Köhler, S. E. Moya, S. Leporatti, C. Bitterlich, E. Donath, *Eur. Biophys. J.* **2007**, *36*, 337.
[16] L. Hosta-Rigau, R. Chandrawati, E. Saveriades, P. D. Odermatt, A. Postma, F. Ercole, K. Breheney, K. L. Wark, B. Städler, F. Caruso, *Biomacromolecules* **2010**, *11*, 3548.
[17] E. Donath, G. B. Sukhorukov, F. Caruso, S. A. Davis, H. Möhwald, *Angew. Chem. Int. Ed.* **1998**, *37*, 2201.
[18] A. R. Battle, S. M. Valenzuela, A. Mechler, R. J. Nichols, S. Praporski, I. L. di Maio, H. Islam, A. P. Girard-Egrot, B. A. Cornell, J. Prashar, F. Caruso, L.L Martin, D. K. Martin, *Adv. Funct. Mater.* **2009**, *19*, 201.
[19] C. Delajon, T. Gutberlet, R. Steitz, H. Möhwald, R. Krastev, *Langmuir* **2005**, *21*, 8509.
[20] T. Hatakeyama, H. Hatakeyama, K. Nakamura, *Thermochim. Acta* **1995**, *253*, 137.
[21] K. Köhler, D. G. Shchukin, H. Möhwald, G. B. Sukhorukov, *J. Phys. Chem. B.* **2005**, *109*, 18250.
[22] T. J. Madera-Santana, M. Misra, L. T. Drzal, D. Robledo, Y. Freile-Pelegrin, *Polym. Eng. Sci* **2009**, *49*, 1117.
[23] E. Fernández, R. Hernández, M. T. Cuberes, C. Mijangos, D. López, *J. Polym. Sci. B* **2010**, *48*, 2403.
[24] L. Yang, A. Guiseppi-Wilson, A. Guiseppi-Elie. *Biomed. Microdevices* **2011**, *13*, 279.
[25] L. Dauginet, A. S. Duwez, R. Legras, S. Demoustier-Champagne, *Langmuir* **2001**, *17*, 3952.
[26] A. A. Mamedov, N. A. Kotov, *Langmuir* **2000**, *16*, 5530.
[27] S. S. Ono, G. Decher, *Nano Lett.* **2006**, *6*, 592.
[28] Y. Ma, J. Sun, J. Shen, *Chem. Mater.* **2007**, *19*, 5058.
[29] A-N. Dirieh Egueh, B. Lakard, P. Fievet, S. Lakard, C. Buron, *J. Colloid Interface Sci.* **2010**, *344*, 221.
[30] A. A. Antipova, G. B. Sukhorukov, *Adv. Colloid Interface Sci.* **2004**, *111*, 49.
[31] R. v.Klitzing, H. Möhwald, *Macromolecules* **1996**, *29*, 6901.
[32] R. A. Ghostine, J. B. Schlenoff, *Langmuir* **2011**, *27*, 8241.
[33] P. Roger, C. Mattisson, A. Axelsson, G. Zacchi, *Biotechnol. Bioeng.* **2000**, *69*, 654.
[34] P. Yin, C. J. Burns, P. D. J. Osman, B. A. Cornell. *Biosens. Bioelectron.* **2003**, *18*, 389.
[35] D. M. Nikolelis, M. Mitrokotsa. *Biosens. Bioelectron.* **2002**, *17*, 565.
[36] G. B. Sukhorukov, E. Donath, H. Lichtenfeld, E. Knippel, M. Knippel, A. Budde, H. Möhwald, *Colloids Surf. A.* **1998**, *137*, 253.
[37] B. Stidder, G. Fragneto, R. Cubitt, A. V. Hughes, S. J. Roser, *Langmuir* **2005**, *21*, 8703.
[38] B. Stidder, G. Fragneto, S. J. Roser, *Langmuir* **2005**, *21*, 9187.
[39] H. P. Wacklin, *Curr. Opin. Colloid Interface Sci.* **2010**, *15*, 445.